# A limit on the number density of bright z  7 galaxies

Elizabeth R. Stanway, Malcolm N. Bremer, Valentina Squitieri, Laura S. Douglas, Matthew D. Lehnert

Mon. Not. R. Astron. Soc. **386,** 370–376 (2008) doi:10.1111/j.1365-2966.2008.13030.x

# A limit on the number density of bright $z \approx 7$ galaxies

Elizabeth R. Stanway,[1⋆] Malcolm N. Bremer,[1] Valentina Squitieri,[1]
Laura S. Douglas[1,2] and Matthew D. Lehnert[3]

[1]*H H Wills Physics Laboratory, Tyndall Avenue, Bristol BS8 1TL*
[2]*School of Physics, Stocker Road, Exeter EX4 4QL*
[3]*Laboratoire d'Etudes des Galaxies, Etoiles, Physique et Instrumentation GEPI, Observatoire de Paris, Meudon, France*

Accepted 2008 January 28. Received 2008 January 28; in original form 2007 October 4



**ABSTRACT**

We present a survey of bright optical dropout sources in two deep, multiwavelength surveys comprising 11 widely separated fields, aimed at constraining the galaxy luminosity function at $z \approx 7$ for sources at 5–10 $L^*$ ($z = 6$). Our combined survey area is 225 arcmin$^2$ to a depth of $J_{\rm AB} = 24.2$ ($3\sigma$) and 135 arcmin$^2$ to $J = 25.3$ ($4\sigma$). We find that infrared data longwards of 2 μm are essential for classifying optical dropout sources, and in particular for identifying cool Galactic star contaminants. Our limits on the number density of high-redshift sources are consistent with current estimates of the Lyman break galaxy luminosity function at $z = 6$.

**Key words:** galaxies: evolution – galaxies: high-redshift – galaxies: starburst.

## 1 INTRODUCTION

Direct observations of galaxies at very high redshift can cast light on the details of structure formation and early galaxy evolution. In recent years, the most commonly observed tracer of star formation at high redshift has been the Lyman break galaxy (LBG) population (Steidel et al. 1999). These sources are selected photometrically based on a spectral feature interpreted as being the $\lambda_{\rm rest} = 1215.67$ Å Lyman break. Neutral hydrogen along the line of sight leads to a forest of redshifted Lyman $\alpha$ absorption lines, blue continuum flux is suppressed and a galaxy will exhibit red colours in a pair of filters bracketing the break. Depending on the relative depth of the imaging in different bands, the galaxy will be seen to fall in magnitude between the red and bluewards bands, or even to drop below the detection limit. As a result, LBGs are often termed 'drops' or 'dropouts' and their approximate redshift is determined by the band bluewards of the break. Hence, 'U' and 'G' drops lie at $z \approx 3$ and 4 (Steidel et al. 1999), 'V' and 'R' drops at $z \approx 5$ (Lehnert & Bremer 2003; Giavalisco et al. 2004b) and 'I' drops at $z \approx 6$ (Stanway, Bunker & McMahon 2003; Bouwens et al. 2006).

The use of LBG samples to study star formation at ever increasing redshifts has recently encountered a practical barrier. At $z \approx 7$, the Lyman break is redshifted to 1 μm, a spectral region with poor sensitivity in both optical CCD detectors and near-infrared (near-IR) instruments. Photometry in the relatively broad photometric filters used longwards of 1 μm effectively smears out the signatures of sharp-sided spectral features such as the Lyman break, making them difficult to distinguish from more gradual spectral features such as a Balmer break or molecular absorption in low-redshift sources. The small field of view, high background, low sensitivity and low multiplexing of current near-IR spectrographs further complicate the follow-up of LBG candidates.

Sensitive, wide-format near-IR imagers and multi-object spectrographs on the largest telescopes offer potential for $z = 7$ LBG searches, identifying bright near-IR sources that drop in the optical bands (as discussed below in Section 2). Such surveys require knowledge of the $z = 7$ luminosity function in order to estimate the required survey depth in a given area. High contamination rates in optical-dropout samples also complicate such surveys. While the most promising candidates will always require spectroscopic follow up, it is clearly necessary to develop strategies for minimizing the number of contaminating lower redshift sources from photometry alone. An important tool for fulfilling these requirements is the *Spitzer Space Telescope*, which images at IR wavelengths. However, the 85-cm aperture of *Spitzer* and 1.2 × 1.2 arcsec$^2$ pixel of its IRAC instrument lead to blending and confusion issues at faint limits ($m_{\rm AB} > 24$). Existing deep field surveys incorporate sensitive imaging at wavelengths from 4000 Å to 8 μm (the four bands of the IRAC instrument). As a result, they can provide a first constraint on the surface density of bright galaxies at very high redshifts, and a test of the ability of *Spitzer* to distinguish genuine $z > 7$ sources from lower redshift contaminants.

In this paper, we present an analysis of two multiwavelength data sets, identifying and classifying optical-dropout sources in 11 widely separated fields, averaging across cosmic variance. In Section 2, we discuss the colour selection criteria which isolate high-redshift galaxies. In Sections 3 and 4, we apply such criteria to the ESO Remote Galaxy Survey and the Great Observatories Origins Deep Survey, respectively, and consider the resulting candidate sources. Finally, in Section 5, we discuss the implications of this analysis for both the $z = 7$ LBG luminosity function and future wide-area near-IR survey.

⋆E-mail: e.r.stanway@bristol.ac.uk

All magnitudes in this paper (optical and IR) are quoted in the AB system (Oke & Gunn 1983). We use a flat Universe with $\Omega_\Lambda = 0.7, \Omega_M = 0.3$ and $H_0 = 70\,h_{70}\,\mathrm{km\,s^{-1}\,Mpc^{-1}}$.

## 2 COLOUR SELECTION OF $z = 7$ GALAXIES

We employ the Lyman break technique, identifying sources that drop dramatically in flux between the reddest optical filter ($z$ band) and the bluest commonly used filter in the IR ($J$ band). This criterion is sensitive to galaxies at $z > 7$, at which redshift flux longwards of the Lyman break becomes shifted beyond the optical. Given that the mean transmitted flux fraction through the Lyman $\alpha$ forest at $z \approx 6$ is less than 5 per cent (Songaila & Cowie 2002) and may well fall to zero between $z \approx 6.0$ and 6.5 (Fan et al. 2006), genuine high-redshift candidates are expected to have no detectable flux in any optical band, as Fig. 1 illustrates.

However, other well-known populations exhibit similar colours, with relatively high number densities, rendering the search for high-redshift galaxies akin to the search for a needle in a haystack. The 4000 Å Balmer break in old galaxies at $z \approx 2$ could potentially be mistaken for a Lyman break at $z > 7$, although such galaxies are likely to be detected in sufficiently deep optical imaging. Cool late-type stars, particularly class L and T dwarfs, are also optically faint, but potentially bright in the near-IR (e.g. Patten et al. 2006). In order to identify all or most interlopers, we require four broad-band colour selection criteria in addition to the optical non-detection. These are illustrated in Figs 2 and 3. Cuts in the $J - K$ or $J - 3.6\,\mu$m will effectively exclude the majority of cool $T$ class stars which are blue in these colours. Since these two colours are highly correlated, with most of the colour difference arising from $J - K$, strictly only one is necessary. However, given the challenge of observing in the thermal IR from the ground, it is often possible to survey large areas to deeper limits in 3.6 μm with *Spitzer*/IRAC than in $K$ from the ground, allowing the $J - 3.6\,\mu$m colour to provide stronger limits in the case of faint or undetected objects.

The true utility of the IR, however, lies at longer wavelengths. As Fig. 3 illustrates, a further requirement that sources are flat or slightly

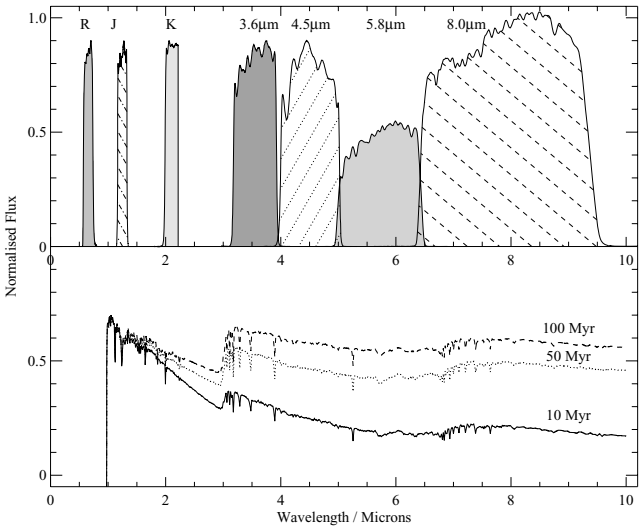


**Figure 1.** The filters and model spectra considered in this work. The filter response curves of the ESO/VLT $R$ band, Mauna Kea Observatories $J$ and $K$, and *Spitzer*/IRAC channels, span the rest-frame UV and optical spectra of galaxies at high redshift. We use the models of Maraston (2005) shown here placed at $z = 7$.

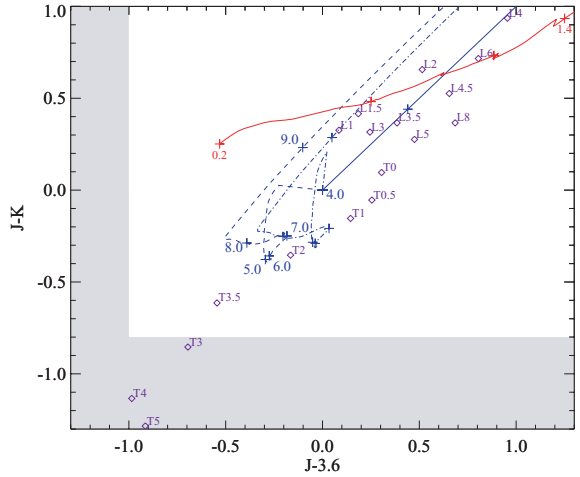


**Figure 2.** The near-IR colours of optical dropout populations. The blue lines show the redshift evolution of young starburst galaxies (solid – flat in $f_\nu$; dashed – 50 Myr after start of burst, dot–dash – 100 Myr). The red line indicates the redshift evolution of an elliptical galaxy formed at $z = 5$ with exponentially decaying star formation ($\tau = 0.5$ Gyr). The models of Maraston (2005) are used throughout. The purple diamonds indicate the measured colours of cool Galactic stars (Patten et al. 2006). Shaded regions are excluded by our colour selection criteria.

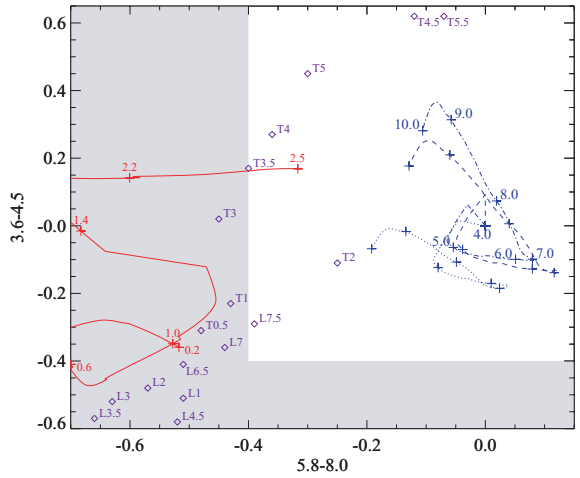


**Figure 3.** The colours of optical dropout sources in the *Spitzer*/IRAC wavebands. For explanation of lines and symbols, see Fig. 2.

red in the *Spitzer*/IRAC wavebands is likely to exclude some low-redshift galaxies and the majority of $L$ class stars, which separate neatly from the predicted colours of young starburst galaxies at $z > 7$. Unfortunately, it is impossible to exclude some late $L$ and early $T$ class stars while allowing for photometric and intrinsic scatter in the high-redshift galaxy population.

A final source of contamination potentially arises from mature (>1 Gyr old), highly reddened galaxies at intermediate redshifts. Such sources have been identified in deep samples selected at 3.6 μm and identified as optical dropouts (e.g. Stern et al. 2006; Rodighiero et al. 2007) and have extreme colours in both $J - K$ and $K - 3.6\,\mu$m, as opposed to mature galaxies at high redshift (which can have dramatic $J - 3.6\,\mu$m colours), but have near-zero colour in $J - K$. While it is impossible to eliminate such sources from a sample without also rejecting highly reddened, mature galaxies (which show

a Balmer break) at $z > 8$, any galaxies with such colours must be treated with caution. Given the scarcity of very high-redshift galaxies, a Bayesian analysis of the redshift likelihood distribution is likely to favour the low-redshift identification.

## 3 THE ESO REMOTE GALAXY SURVEY

### 3.1 Survey outline

The ESO Remote Galaxy Survey (ERGS, Douglas et al, in preparation) is aimed at identifying $z > 5$ LBGs in the same deep imaging fields imaged by the ESO Distant Cluster Survey (EDisCS, White et al. 2005). Each of 10 widely separated fields was surveyed in the optical (*VRIZ*) using the FORS2 instrument on the Very Large Telescope (VLT), in the near-IR ($JK_s$) using Son of ISSAC (SOFI) on the New Technology Telescope (NTT) and in the IR (3.6, 4.5, 5.8 and 8.0 μm) using IRAC on *Spitzer*. Typical depths reached were 27.8 in the *V* band, 27.4 in *R*, 26.6 in *I*, 25.9 in *Z*, 24.6 in the *J* band and 23.8 in *K* ($2\sigma$, 2 arcsec apertures). Typical seeing was 0.6–0.8 arcsec in the ground-based data. In the IRAC bands, the $2\sigma$ limiting depths were measured in a 4.5 arcsec aperture and were 25.1 at 3.6 μm, 25.2 at 4.5 μm, 23.0 at 5.8 μm and 22.9 at 8.0 μm. For full details of the data see White et al. (2005) and Douglas et al (2008). For the purposes of identifying optical dropouts, we required full 10 band photometric coverage, yielding a total survey area of 225.1 arcmin$^2$ (after removing regions with high-background noise in the near-IR). Objects were selected in the *J* band using the SExtractor software package (Bertin & Arnouts 1996) and their fluxes measured at the centroid of the *J*-band detection in each band using the IDL 'Aper' routine. For initial detection, we required that an area of four contiguous pixels exceeded the background by at least 1.5 standard deviations, resulting in a basic photometry catalogue highly complete for unresolved and low surface brightness sources, but also highly contaminated by spurious objects at the faint end. Photometry was measured in 2 arcsec apertures in the optical and near-IR and in larger 4.5 arcsec apertures in the *Spitzer*/IRAC bands in order to optimize signal-to-noise ratio (S/N) for our unresolved sources. The astrometry in the optical images and near-IR images was found to be precise to better than 0.1 arcsec (half a pixel) and to within 0.6 arcsec in the IRAC bands. We find that adding an uncertainty of 0.35 arcsec (half the seeing disc) to the location of the *J*-band centroid for our compact, low S/N objects have the effect of introducing an additional error to the photometry with a standard deviation of 0.04 mag at the faint limit of our survey. This is negligible when added in quadrature with the Poisson noise and statistical uncertainty in the background at the same magnitude.

A refined catalogue was constructed of objects with *J*-band detections ($>3\,\sigma$), but no detection at $2\,\sigma$ in each of the *V*, *R*, *I* and *Z* bands. The *V*, *R* and *I*-band imaging was combined to create a single optical image (reaching a limiting magnitude better than 28.5 in each field) and a further non-detection required in this image. Magnitudes were not corrected for lensing. However, we note that the mean weak lensing effect across these fields is to brighten the observed magnitudes by 0.1 mag (Clowe et al. 2006) compared to their intrinsic magnitudes. Candidate high-redshift sources satisfy $J_{\rm AB} < 24.2$ (3–4$\sigma$ depending on field) after correction for aperture losses. Each candidate was inspected by eye and obvious data artefacts excluded, leaving a sample of 35 candidate sources for further inspection.

By definition our target sources may only be bright in a single band, and this measurement is therefore susceptible to spurious sources in the detection band. In order to estimate the probability that our optical-dropout sources are not merely spurious detections of peaks in the random background noise, we repeated the analysis, inverting the *J*-band imaging in the ERGS fields and determining the number of negative noise peaks that would have been detected as objects to our limit if they were instead positive signals.

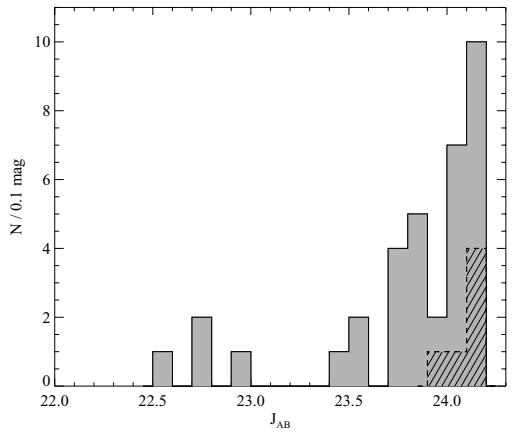


**Figure 4.** The expected magnitude distribution of spurious sources due to fluctuations in background noise (hatched), compared with the distribution of optical-dropout candidates (shaded). The number of spurious sources is based on detection of the total number of negative noise peaks in the *J*-band imaging as a function of magnitude.

After discounting obviously spurious detections (cosmic ray subtraction residuals, regions of extended noise and depressions in the background in the wings of bright emission objects), we find six genuine noise peaks in the 225.1 arcmin$^2$ survey area which would have been mistaken for dropout sources if positive. Their magnitude distribution, together with that of the optical dropout candidates is shown in Fig. 4. Making the assumption that depressions in the background of this kind are statistically as likely as positive fluctuations which would reach the photometric catalogue, we estimate that a fraction of 17 per cent of our candidate sample, biased towards the faint end, may be spurious detections. We note that none of the spurious detections are brighter than '$J = 23.9$' (assuming positive flux) and that none of them coincide with source detections in any of the other nine bands surveyed.

Given the faint limits of our data, and the relatively broad point spread function (PSF) of the *Spitzer Space Telescope* in the IRAC bands, we also test the probability that random apertures placed on the 3.6 μm images that form part of the ERGS survey coincide with IR-detected sources. Placing 300 apertures randomly in each of the 10 survey fields, we find that 39 per cent of photometric apertures are expected to encounter flux from contaminating sources equal to a $3\sigma$ peak in the background level (corresponding to a detection of $J = 24.2$).

### 3.2 $z = 7$ candidates

This analysis yielded a total of 35 optical dropout sources, distributed across 10 equally sized fields. Of these, the most densely populated field contained seven candidate objects and the sparsest field only one candidate.

The IR colours of each candidate were subjected to detailed analysis to determine the most likely identification: $z > 7$ galaxy, lower redshift galaxy or Galactic star. Of the 35 dropout sources, 15 were blended at the resolution of *Spitzer*/IRAC and cannot be studied further, consistent with the expected 13.7 confused sources given

**Table 1.** Photometry of the remaining sources satisfying the colour selection criteria for high-redshift ($z > 7$) galaxies in the ERGS and GOODS survey areas. The Opt− $J$ indicates an optical to near-IR colour, measured from the *VRI*-combined image for the first object, and from the *F*435*W* band in the latter two candidates. The S/N of each source in the $J$ band is shown in brackets.

| RA and Dec. (J2000) | $J_{AB}$ | Opt− $J_{AB}$ | $Z_{AB} - J_{AB}$ | $J_{AB} - K_{AB}$ | $(J - 3.6\ \mu m)_{AB}$ | $(3.6–4.5\ \mu m)_{AB}$ | $(5.8–8.0\ \mu m)_{AB}$ |
|---|---|---|---|---|---|---|---|
| 10 54 41.35 −12 44 07.3 | $23.61 \pm 0.26$ (3.8) | >4.9 | >2.1 | <0.15 | $-0.10 \pm 0.31$ | $-0.36 \pm 0.27$ | – |
| 03 32 25.22 −27 52 30.7 | $24.73 \pm 0.19$ (5.2) | >3.3 | >1.8 | $1.81 \pm 0.22$ | $3.35 \pm 0.20$ | $0.45 \pm 0.06$ | $-0.14 \pm 0.24$ |
| 03 32 16.81 −27 49 07.5 | $24.79 \pm 0.22$ (4.5) | >3.2 | >2.1 | $1.57 \pm 0.25$ | $2.99 \pm 0.23$ | $0.05 \pm 0.06$ | $-0.36 \pm 0.24$ |

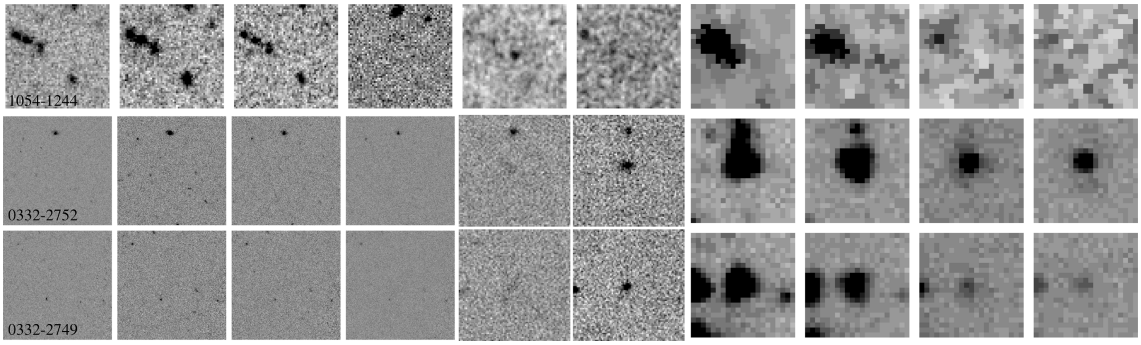


**Figure 5.** Postage stamp images of the three candidate sources listed in Table 1. Boxes are 12 arcsec to a side. In the case of 1054–1244, the bands shown are $V$, $R$, $I$, $Z$, $J$, $K$, [3.6], [4.5], [5.8], [8.0]. In the remaining two cases $V$, $R$, $I$, $Z$ is replaced by $b$, $v$, $i'$, $z'$. While all three sources satisfy the colour selection criteria, their behaviour in the IR is quite different.

Poisson noise in the small number statistics. Deblending was not attempted since, at these faint magnitudes, errors in the resultant flux measurement would be dominated by uncertainty in the colour and isophotal profile of the confusing sources. The remaining 20 optical dropouts had clean IR photometry. Of these, two sources were eliminated because of their blue $J - K$ colours ($J - K < -0.8$), and a further eight were rejected as too blue in the $J - 3.6\ \mu m$ colour ($J - 3.6\ \mu m < -1.0$). The most likely identification of these sources is that they are T dwarf stars at moderate heliocentric distances (see Section 5.1). Finally, a further nine candidates were eliminated from the sample as their colour (or the $2\sigma$ limit on the colour) satisfied $3.6–4.5\ \mu m < -0.4$. These candidates are considered most likely to be either L-class dwarfs or old galaxies at intermediate redshift.

Thus, only one candidate of 20 sources studied has colours satisfying the colour criteria in Figs 2 and 3. The colours of this source are given in Table 1 and it is shown in Fig. 5. The remaining source has a magnitude $J = 23.6$ suggesting that it is statistically unlikely to be a chance detection of a spurious noise peak. While the source satisfies our formal selection criteria, its colours are close to the bluewards cut-off in 3.6–4.5 μm colour. This colour is consistent with that of an early T dwarf and, given the photometric errorbars on this faint source, marginally consistent with identification as a $z > 7$ source in some star formation histories. Hence, in our 225.1 arcmin$^2$ survey area we find an upper limit of 1.43 sources, assuming a similar contamination fraction for the IR-blended fraction, lying at $z > 7$ and a more likely limit of fewer than one high-redshift galaxy to a depth of $J_{AB} = 24.2$ ($3\sigma$).

## 4 THE GOODS SURVEY

### 4.1 Survey outline

The Great Observatories Origins Deep Survey (GOODS, Giavalisco et al. 2004a) is a publicly available data set comprising observations from major ground- and space-based observatories. We make use of the r1.1 photometric catalogue release which comprises the results of imaging in the *F404W* ($b$), *F606W* ($v$), *F814W* ($i'$) and *F850LP* ($z'$) filters of the Advanced Camera for Surveys on the *Hubble Space Telescope* (*HST*/ACS). We supplement this with the $J$- and $K_s$-band data obtained as part of the GOODS programme at the VLT (Vanzella et al. 2006) and with *Spitzer*/IRAC data obtained as part of the GOODS Legacy Programme (PI: Mark Dickinson). As in the analysis in Section 3, we measured photometry in 2 arcsec apertures in the optical and near-IR, and in 4.5 arcsec apertures in the IR. In these large apertures, we require non-detection to limiting magnitudes of 27.8 in $b$ and $v$, 27.0 in $i'$ and 26.8 in the $z'$ band and also non-detection in visual inspection of the images (since compact sources can be detected to more sensitive limits in the high-resolution space-based data). The near-IR imaging reaches $2\sigma$ limits of $J = 25.8$ and $K_s = 25.2$, while the $2\sigma$ limiting depths were 27.1 at 3.6 μm, 26.6 at 4.5 μm, 24.8 at 5.8 μm and 8.0 μm.

We restrict our analysis to the GOODS-South field and survey a total of 135.0 arcmin$^2$ with full 10 band photometric coverage. As before, we train our catalogue in the $J$ band and measure the flux at the near-IR location in $K_s$ and longwards. Optical counterparts are assigned to sources if an *HST*/ACS detection is identified within 1 arcsec of the near-IR centroid. Optical dropout candidates were inspected by eye and spurious detections removed. We limit our catalogue to sources with a $4\sigma$ detection of $J < 25.3$.

As in the case of the ERGS survey fields above, we consider the fraction of confused sources we might expect in the *Spitzer*/IRAC bands through the investigation of randomly placed apertures on the 3.6 μm image. While the IRAC data in the GOODS fields are deeper than in the ERGS fields, the GOODS region was chosen for its low foreground contamination, while the ERGS survey exploits lower redshift cluster fields. Hence, the contamination fraction amongst randomly placed apertures in the GOODS-south field was a slightly lower fraction of 28 per cent coincidence with $3\sigma$ flux from other sources.

### 4.2 $z = 7$ candidates

This analysis yielded a total of 14 optical dropout sources. Of these, four sources (one with $J < 24.2$) are blended at the resolution of *Spitzer*/IRAC and cannot be studied further, consistent with the 3.9 sources expected from pure confusion. A further two sources are too blue in their IR colours to be high-redshift galaxies (i.e. $J - 3.6\,\mu\mathrm{m} < -1.0$), and are tentatively classified as likely T dwarf stars. The remaining eight sources are well detected at 3.6–8.0 μm. However, while their 3.6–4.5 μm colours are consistent with either high- or low-redshift identification, in six cases (two of which have $J < 24.2$) their colours at longer wavelengths are rather blue (5.8–8.0 μm $< -0.4$) suggesting that a low-redshift interloper galaxy interpretation is more likely.

The photometry of the remaining two candidates is given in Table 1. We note that both sources are detected in the $J$ band at >5 sigma, suggesting that they are statistically unlikely to be spurious detections based on our analysis of the ERGS fields discussed above. Both sources are also well detected in the $K$ band, making a chance coincidence of $J$ band noise with a *Spitzer*/IRAC source unlikely. Both sources show a red spectrum leading to near equal $J - K$ and $K - 3.6\,\mu$m colours. As discussed in Section 2, this may suggest either identification as a high-redshift candidate or as a reddened mature galaxy at intermediate redshifts. Given the scarcity of high-redshift galaxies, the latter explanation is the more likely. Hence, in our survey area of 135 arcmin$^2$ we find an upper limit of 2.8 sources (accounting for the fraction of IR-blended sources) lying at $z > 7$ and a more likely limit of fewer than one high-redshift galaxy to a depth of $J_{\mathrm{AB}} = 25.3$ ($4\sigma$).

## 5 DISCUSSION

### 5.1 The surface density of L and T dwarf stars

Given the difficulty in unambiguously classifying extremely red sources on the basis of photometry alone, it is instructive to determine whether the red population identified in this work represents an excess over predicted number counts for low-redshift objects. Specifically, given that early to mid-T dwarfs are expected to be our most significant contaminant on the basis of their observed IR colours (Patten et al. 2006), it is useful to calculate the surface density of T dwarf stars.[1]

The number of T dwarf stars with spectroscopic confirmation in the literature remains small (see Looper, Kirkpatrick & Burgasser 2007, and references therein), although this number is increasing rapidly due to follow-up of photometrically identified candidates in wide-area surveys such as the Sloan Digital Sky Survey (SDSS) (e.g. Chiu et al. 2006). Looper et al. (2007) report a lower limit to the surface density of T dwarfs (T1–T8) of $3 \times 10^{-3}\,\mathrm{pc}^{-3}$ based on a catalogue of known sources within 10 pc of the sun, although they note that they may be considerably incomplete due to the non-uniformity of the input surveys. A more complete analysis of the surface density of T dwarfs was performed in the SDSS DR1/Two-Micron All-Sky Survey overlap region by Metchev et al. (2007), using Monte Carlo simulation to estimate the effect of selection functions in both surveys. They estimate a volume density of class T0–T8 dwarfs of $(7.0 \pm 3.1) \times 10^{-3}\,\mathrm{pc}^{-3}$.

Given the typical absolute magnitude of a class T3 star ($J_{\mathrm{AB}} = 15.3$, Metchev et al. 2007), we would be able to detect such a star between a distance of 57 pc (closer than which our detectors saturate) and 603 pc (for a limit of $J = 24.2$) or 1000 pc (for $J = 25.3$). Given that these distances are well within the scaleheight of the disc, we make the assumption that the volume density of T stars is constant in this range. From this, we estimate a total enclosed volume for early to mid-T stars of 2224 pc$^3$ in our shallow survey and 3796 pc$^3$ in our deep survey area. This corresponds to a predicted $16 \pm 7$ T dwarf stars in our shallow survey and $27 \pm 12$ T stars in our deep survey.

We compare this with the number of sources in our data set classified as likely T dwarf interlopers on the basis of their IR colours. To a limit of $J = 24.2$ in the 11 survey fields (ERGS+GOODS), we identified a total of 10 sources as likely T dwarf interlopers due to very blue colours in the *Spitzer*/IRAC bands. Assuming an equal ratio of T dwarf candidates to $z$ drops amongst the IR-confused sources, this yields a tentative volume density of $(7.9 \pm 0.2) \times 10^{-3}\,\mathrm{pc}^{-3}$.

We note that this is at the high end of the volume density estimates discussed above, but is consistent within the errorbars, given that this is a near-IR selected sample. Given the huge field to field variation in the number density of red sources in our shallow survey, and the still significant uncertainty in the surface density of local T dwarfs, our results are consistent with at least half of our identified $z$ drops being T dwarf stars.

Our results from the deep survey area are less consistent with published volume densities for interlopers, with just two optical-dropout sources identified as good T dwarf candidates to a depth of $J = 25.3$. We note that our deep survey is confined to a single region, the GOODS-South field, which also appears to be deficient in $z$-band dropout sources at $J < 24.2$ compared to the mean of our ERGS survey fields, and that there is a factor of 6 in surface density between our richest and sparsest fields. It is possible that the GOODS-South sightline probes a void in the local T dwarf distribution, or that the local density is a poor approximation at increasing heliocentric (and, in this case, galactocentric) distance. Given the very small solid angle subtended by our fields, it is likely that multiple sightlines through the Galactic disc and halo will be required to determine the mean volume density of such sources as a function of Galactocentric coordinate.

### 5.2 Implications for the $z = 7$ luminosity function

While the detection of zero or very few dropout candidates to these relatively shallow limits is not entirely surprising, it is interesting to consider possible constraints on the luminosity function that may be derived from this result.

The typical luminosity of the LBG population, $M^*$, is known to evolve with cosmic time, becoming fainter with increasing redshift (Bouwens et al. 2007). The highest redshift sample for which the luminosity function has been well constrained is the $i'$-dropout population at $z = 6$. Bouwens et al. (2007) found that such a population is described by a Schecter function with $M *_{UV} = -20.2 \pm 0.2$, $\alpha = -1.7$ and a surface density $\phi^* = (1.4 \pm 0.5) \times 10^{-3}\,\mathrm{Mpc}^{-3}$.

Given no evolution in the shape and comoving volume density normalization luminosity function between $z = 6$ and 7 (914 and 748 Myr after the big bang), we can predict the expected number of sources at the bright end of the luminosity function. Our colour selection as described in Section 2 is, in theory sensitive over a broad redshift range, from $z = 6.5$ to 10. However, in an apparent magnitude-limited sample, the redshift sensitivity function will be biased towards sources at lower redshift, particularly for a luminosity function with a steep faint end. Our limiting magnitude is 1.6 mag fainter at $z = 10$ than at $z = 6.5$, a dramatic difference at $> L^*$. We therefore calculate our survey volume using the effective

[1] We do not discuss the density of L dwarfs since an essentially unknown fraction, varying with distance, of these will be excluded by the optical non-detection criterion.

volume method after Steidel et al. (1999), accounting for the different limiting luminosity in each $\Delta z = 0.01$ redshift shell, using the prescription

$$V_{\rm eff}(m) = \int {\rm d}z\; p(m, z)\, \frac{{\rm d}V}{{\rm d}z},$$

where $p(m, z)$ is the probability of detecting a galaxy at redshift $z$ and apparent $z$-band magnitude $m$, given the luminosity function and galaxy colour (randomly perturbed by an error of 0.3 mag at the faint limit of the survey), and ${\rm d}z\, \frac{{\rm d}V}{{\rm d}z}$ is the comoving volume per unit solid angle in a slice d $z$ at redshift $z$.

Given the parameters of the $z = 5.9$ luminosity function discussed above (Bouwens et al. 2007), we find that our shallow survey is sensitive to 8.0 per cent of the total volume enclosed between $z = 6.5$ and 10.0 per unit area to the limiting luminosity of the faintest object in the sample, while the deep survey selection is sensitive to 16.5 per cent of the same volume. We note that if we were to adopt instead the tentative value of $M^*$ proposed by Bouwens et al. (2007) for $z = 7$, we would survey an effective volume only 4.5 and 9 per cent of the total volume enclosed by the redshift range sensitivity range.

In our shallow sample reaching $J = 24.2$, we survey an effective volume of $1.0 \times 10^6$ Mpc$^3$ and reach a typical limiting magnitude (at $z = 7$) of $M_{UV} = -22.7$. Assuming no evolution in the high-redshift LBG luminosity function, we are sensitive to galaxies brighter than $10\,M^*$ (given the $z = 6$ value for $M^*$). Our detection of no good candidates in the combined GOODS+ERGS sample is consistent with the predicted 0.001 galaxies.

While this is not unexpected it is interesting to note that recent evidence from $z > 5$ galaxy populations have suggested that the universe at earlier times was a more vigorously active place. The evolution in size of LBGs, together with their more slowly evolving star formation rates implies that star formation density rises with increasing redshift (Verma et al. 2007). The identification of old stellar populations in $z = 6$ galaxies (Eyles et al. 2005) also implies that starburst activity must have been rapid and intense at early times. Hypothetical luminosity functions for primordial starbursts (which have a top-heavy initial mass function and a higher light-to-mass ratio than more conventional stellar populations) imply that a factor of 100 or more increase might be seen in the number density of ultraviolet (UV)-luminous sources at $z > 7$ (Barton et al. 2004). The number density of $z = 7$ candidates in our combined ERGS+GOODS survey area provides a firm upper limit on the bright end of the luminosity function, confirming that it inhabits the expected region of parameter space.

Our deeper sample reaches $J = 25.3$ or a typical limiting magnitude (at $z = 7$) of $M_{UV} = -21.6$. Assuming no evolution in the high-redshift LBG luminosity function, we are sensitive to galaxies brighter than $3.6\,M^*$. In our effective survey volume, $7.7 \times 10^5$ Mpc$^3$, we might expect to observe 2.4 galaxies, consistent with our detection of up to two good candidates. This is sufficient to rule out the most optimistic predictions for metal-free stellar populations at $z > 7$ (see Barton et al. 2004). The upper limits derived from our analysis are consistent with the measured LBG luminosity function at $z = 6$, and suggest that the volume density of luminous (brighter than $M^*$) galaxies remains approximately constant (if both our candidates are real $z > 7$ galaxies) or decreases (if one or more is not real) with increasing redshift rather than increasing.

Bouwens et al. (2004) estimated the surface density of optical dropout sources in the *Hubble Ultra Deep Field* (HUDF) and identified four likely candidates to a depth of $H_{\rm AB} = 27.0$ (as opposed to eight predicted $z = 7$ galaxies based on the $i'$-drop luminosity function). Given a spectrum flat in $f_\nu$ (as appropriate for young starbursts), this is equivalent to two magnitudes deeper than our limit in the GOODS fields and the area of their survey was only 4 per cent of that discussed here. This would imply an expected $0.5\ z = 7$ galaxies meeting our deep survey criteria. While we determine an upper limit of two galaxies at $z > 7$ in our deep survey, our more realistic expectation is that neither is likely to lie at high redshift. The confirmation of one or zero sources would confirm that the HUDF is not significantly underabundant compared with other sightlines at the same redshift.

Given the varied colour selections employed by different authors, fair comparisons are difficult. We note that we would have rejected the majority of massive $z > 4$ galaxy candidates proposed in the GOODS-South by Dunlop et al. (2007) due to the presence of flux in the observed frame optical or as below the reliable detection limit in the $J$ band. By contrast the requirement of Rodighiero et al. (2007) that their candidates be fainter than $K_{\rm s} = 23.5$ would have excluded a number of the candidate galaxies presented here. Their selection method, based on a flux-limited 3.6 μm sample, may effectively select massive galaxies at these redshifts, and yet is likely to suffer incompleteness due to both confusion and insensitivity to young, starbursts (which are highly stochastic and dominate the number counts in high-redshift LBG samples Verma et al. 2007). Hence, the optical-dropout survey presented here is complementary to other $z > 7$ surveys.

### 5.3 Implications for Future Surveys

In the next few years, the United Kingdom Infra-Red Telescope Infrared Deep Sky Survey (UKIDSS) Ultra Deep Survey (UDS) will survey an area of 0.8 deg$^2$ to $K_{\rm AB} \approx 25$ and will incorporate a search for high-redshift galaxies. Our deep survey probes 12.5 per cent of this area and finds at most two candidates which might require spectroscopic follow up, consistent with 16 potential $z = 7$ candidates in the full volume of the UDS – a feasible number given a reasonable investment of large telescope time. This modest number of galaxies is largely independent of evolution in the faint-end slope of the luminosity function, since the selection is truncated well above $M^*$. Given the $z = 6$ luminosity function, perhaps seven of the candidate galaxies identified in the UDS might be expected to lie at high redshift, although continued evolution in $M^*$ with increasing redshift potentially reduces this number still further. It is clear that, even with exceptionally deep auxiliary data bluewards and redwards of the selection bands, the ratio of candidates to genuine galaxies in a photometric sample is likely to be at least 2.3:1.

However, as the analysis in this paper makes clear, the number of contaminant sources in samples derived from optical/near-IR photometry alone is likely to be much higher. Depth-matched imaging in the IR wavebands of *Spitzer*/IRAC is essential for reducing the number of near-IR photometric candidates (which in the UKIDSS UDS could exceed a hundred) to a more practical number for expensive follow-up observations.

Wide-field IR imagers currently being commissioned, such as Hawk-I on the VLT, are likely to revolutionize this field, making $z \geqslant 7$ as accessible to observers as $z < 6$ at the current time. However, the fundamental requirement that auxiliary observations at longer wavelengths are obtained above the atmosphere will limit their utility for high-redshift surveys after the inevitable decline of IRAC on the *Spitzer Space Telescope* and until its eventual replacement by the *James Webb Space Telescope*.

One prospect for the hiatus period between these two events is to extend the lifetime of *Spitzer* in a 'warm' mode (van Dokkum

et al. 2007). While sensitivity would be lost longwards of 5 μm, the two shortest *Spitzer*/IRAC wavebands provide sufficient spectral leverage to identify the majority of potential contaminants (>80 per cent in this study), and in particular to isolate cool Galactic stars from the galaxy locus. Inevitably the size of the 'haystack' will increase with the loss of the 5.8 and 8.0 μm wavebands. However, the use of a warm *Spitzer* for surveys would provide an archive that would be of use for many years, complementing both existing and future, deep ground-based surveys.

## 6 CONCLUSIONS

The key points presented in this paper can be summarized as follows.

(i) We have identified an analysed sample of $z$ band dropout sources in deep, multiwavelength imaging, considering their suitability as potential $z > 7$ galaxy candidates.

(ii) In an area of 360 arcmin$^2$ (the ERGS+GOODS surveys), we determine a strict upper limit of 1.4 potential $z = 7$ galaxies and a likely limit of zero candidates to $J = 24.2$.

(iii) In an area of 135 arcmin$^2$ (the GOODS survey), we determine a strict upper limit of 2.8 potential $z = 7$ galaxies and a likely limit of no good candidates to $J = 25.3$.

(iv) These results are consistent with current estimates of the luminosity function of LBGs at $z = 6$, for galaxies with $L > 5L^*$.

(v) The use of deep data longward of the $K$ band is extremely valuable if the number of high-redshift candidates from deep surveys such as UKIDSS UDS from unmanageable to reasonable numbers for spectroscopic follow up.

## ACKNOWLEDGMENTS

ERS gratefully acknowledges support from the UK Science and Technology Facilities Council (STFC). Based, in part, on observations made with the NASA/ESA *Hubble Space Telescope*, obtained from the Data Archive at the Space Telescope Science Institute. Also based, in part, on observations made with the *Spitzer Space Telescope*, which is operated by the Jet Propulsion Laboratory, CalTech. We thank the GOODS team for making these high-quality data sets public. Research presented here has benefitted from the M, L and T dwarf compendium housed at DwarfArchives.org and maintained by Chris Gelino, Davy Kirkpatrick and Adam Burgasser. The results from the EDisCS/ERGS fields are based on observations made with European Southern Observatory telescopes under programmes 166.A-0162 and 175.A-0706.

## REFERENCES

Barton E. J., Davé R., Smith J.-D. T., Papovich C., Hernquist L., Springel V., 2004, ApJ, 604, L1
Bertin E., Arnouts S., 1996, A&AS, 117, 393
Bouwens R. J. et al., 2004, ApJ, 616, L79
Bouwens R. J., Illingworth G. D., Blakeslee J. P., Franx M., 2006, ApJ, 653, 53
Bouwens R. J., Illingworth G. D., Franx M., Ford H., 2007, ApJ, 670, 928
Chiu K., Fan X., Leggett S. K., Golimowski D. A., Zheng W., Geballe T. R., Schneider D. P., Brinkmann J., 2006, AJ, 131, 2722
Clowe D. et al., 2006, A&A, 451, 395
Dunlop J. S., Cirasuolo M., McLure R. J., 2007, MNRAS, 376, 1054
Eyles L. P., Bunker A. J., Stanway E. R., Lacy M., Ellis R. S., Doherty M., 2005, MNRAS, 364, 443
Fan X. et al., 2006, AJ, 132, 117
Giavalisco M. et al., 2004a, ApJ, 600, L93
Giavalisco M. et al., 2004b, ApJ, 600, L103
Hawley S. L. et al., 2002, AJ, 123, 3409
Lehnert M. D., Bremer M., 2003, ApJ, 593, 630
Looper D. L., Kirkpatrick J. D., Burgasser A. J., 2007, AJ, 134, 1162
Stanway E. R., Bunker A. J., McMahon R. G., 2003, MNRAS, 342, 439
Maraston C., 2005, MNRAS, 362, 799
Metchev S., Kirkpatrick J. D., Berriman G. B., Looper D., 2007, preprint (arXiv:0710.4157)
Oke J. B., Gunn J. E., 1983, ApJ, 266, 713
Patten B. M. et al., 2006, ApJ, 651, 502
Rodighiero G., Cimatti A., Franceschini A., Brusa M., Fritz J., Bolzonella M., 2007, A&A, 470, 21
Songaila A., Cowie L. L., 2002, AJ, 123, 2183
Steidel C. C., Adelberger K. L., Giavalisco M., Dickinson M., Pettini M., 1999, ApJ, 519, 1
Stern D., Chary R.-R., Eisenhardt P. R. M., Moustakas L. A., 2006, AJ, 132, 1405
van Dokkum P., Cooray A., Labbe I., Papovich C., Stern D., 2007, preprint (arXiv:0709.0946)
Vanzella E. et al., 2006, A&A, 454, 423
Verma A., Lehnert M. D., Förster Schreiber N. M., Bremer M. N., Douglas L., 2007, MNRAS, 377, 1024
White S. D. M. et al., 2005, A&A, 444, 365

This paper has been typeset from a TEX/LATEX file prepared by the author.